Geocarto International
Publication details, including instructions for authors and subscription information:
http://www.tandfonline.com/loi/tgei20

Potentiality of feed-forward neural networks for classifying dark formations to oil spills and look-alikes

Konstantinos Topouzelis [a] , Vassilia Karathanassi [b] , Petros Pavlakis [c] & Demetrius Rokos [b]

[a] Joint Research Centre-EC, Institute for the Protection and Security of the Citizen, Maritime Affairs Unit , Ispra, Italy

[b] Laboratory of Remote Sensing , School of Rural and Surveying Engineering, National Technical University of Athens , Athens, Greece

[c] Hellenic Centre for Marine Research , Athens, Greece

Published online: 19 May 2009.

To cite this article: Konstantinos Topouzelis , Vassilia Karathanassi , Petros Pavlakis & Demetrius Rokos (2009) Potentiality of feed-forward neural networks for classifying dark formations to oil spills and look-alikes, Geocarto International, 24:3, 179-191, DOI: 10.1080/10106040802488526

To link to this article: http://dx.doi.org/10.1080/10106040802488526

Geocarto International
Vol. 24, No. 3, June 2009, 179–191

Taylor & Francis
Taylor & Francis Group

Potentiality of feed-forward neural networks for classifying dark formations to oil spills and look-alikes

Konstantinos Topouzelis[a]*, Vassilia Karathanassi[b], Petros Pavlakis[c] and Demetrius Rokos[b]

[a]*Joint Research Centre–EC, Institute for the Protection and Security of the Citizen, Maritime Affairs Unit, Ispra, Italy;* [b]*Laboratory of Remote Sensing, School of Rural and Surveying Engineering, National Technical University of Athens, Athens, Greece;* [c]*Hellenic Centre for Marine Research, Athens, Greece*

(*Received 11 August 2008; final version received 18 September 2008*)

Radar backscatter values from oil spills are very similar to backscatter values from very calm sea areas and other ocean phenomena. Several studies aiming at oil spill detection have been conducted. Most of these studies rely on the detection of dark areas, which have high Bayesian probability of being oil spills. The drawback of these methods is a complex process, mainly because non-linearly separable datasets are introduced in statistically based decisions. The use of neural networks (NNs) in remote sensing has increased significantly, as NNs can simultaneously handle non-linear data of a multidimensional input space. In this article, we investigate the ability of two commonly used feed-forward NN models: multilayer perceptron (MLP) and radial basis function (RBF) networks, to classify dark formations in oil spills and look-alike phenomena. The appropriate training algorithm, type and architecture of the optimum network are subjects of research. Inputs to the networks are the original synthetic aperture radar image and other images derived from it. MLP networks are recognized as more suitable for oil spill detection.

Keywords: oil spill; neural networks; SAR; pollution; sea

1. Introduction

Oil spills are seriously affecting the marine ecosystem and cause political and scientific concern because they have serious effects on fragile marine and coastal ecosystems. Satellite images can improve the possibilities for the detection of oil spills as they cover large areas and offer an economical and easier way of continuous coast areas patrolling. Synthetic aperture radar (SAR) images have been widely used for oil spill detection. The presence of oil film on the sea surface damps the small waves and drastically reduces the measured backscatter energy, resulting in darker areas in SAR imagery (Kubat *et al.* 1998, Solberg *et al.* 1999, Del Frate *et al.* 2000). However, dark areas may be also caused by other phenomena, called 'look-alikes', such as organic film, grease ice, wind front areas, areas sheltered by land, rain cells, current shear zones, internal waves and up-welling zones.

*Corresponding author. Email: kostas.topouzelis@jrc.it

ISSN 1010-6049 print/ISSN 1752-0762 online

DOI: 10.1080/10106040802488526
http://www.informaworld.com

Several studies aiming at oil spill detection have been implemented (Ziemke 1996, Kubat *et al*. 1998, Solberg *et al*. 1999, Del Frate *et al*. 2000, Fiscella *et al*. 2000, Topouzelis *et al*. 2002, Nirchio *et al*. 2005, Ferraro *et al*. 2006, Karathanassi *et al*. 2006, Perkovic *et al*. 2008). Most of these studies rely on the detection of dark areas, which have a high probability of being oil spills. Any formation on the image which is darker than the surrounding area has a high probability of being an oil spill and needs further examination. Although this process seems to be simple for a human operator, it contains difficulties if semi-automated or automated methods are used. Once the dark areas are detected, classification methods based on Bayesian or other statistical methods are applied to characterize dark areas as oil spills or 'look-alikes'. Characteristics (geometric, surrounding, backscattering, etc.) of spectral and spatial features of the dark area are used to feed the statistical model. Characteristics describe the dark features and can be seen as inputs to the classifiers. For example, an oil spill cannot cover a very big area. On the contrary, a low wind area is expected to be quite big.

Several problems can be faced during the classification phase. Fresh linear oil spills have a weak backscattering contrast relative to their surroundings and thus cannot be easily discriminated. Areas surrounding dark spots can have various contrast values, depending on the local sea state, oil spill type and image resolution. Furthermore, the other phenomena described above are presented as dark areas too. Further classification of the dark areas as oil spills and look-alikes is therefore required. The drawback of the statistical methods is a complex process not fully understood, as it contains several non-linear factors. The development of an inverse model to estimate such parameters turns out to be very difficult.

Neural networks (NNs) have been used to process remote sensing images and have achieved improved accuracy compared with the traditional statistical methods (Kanellopoulos and Wilkinson 1997, Kavzoglu and Mather 2003, Stathakis and Vasilakos 2006, Stathakis and Perakis 2007). Recent work has demonstrated that NNs represent an efficient tool for modelling a variety of non-linear discriminant problems. NNs may be viewed as a mathematical model composed of several non-linear computational elements called neurons, operating in parallel and massively connected by links characterised by different weights (Ziemke 1996, Kanellopoulos and Wilkinson 1997, Del Frate *et al*. 2000).

In the field of oil spill detection, NNs has been firstly used by Ziemke (1996). He studied the ability of several NNs (i.e. Learning Vector Quantization, Feed-forward Backpropagation (BP) networks and Elman–Jordan recurrent networks) to detect dark patches using side looking airborne radar images but no discrimination between oil spills and look-alikes was performed. Later, a feed-forward multilayer perceptron (MLP) to distinguish oil spills from look-alikes in low-resolution SAR images was used by Del Frate *et al*. (2000). Low-resolution images are sufficient for detecting big and old spills, but they are under question for small and fresh oil spills. A first attempt to use full SAR images with NNs for oil spill detection was made by Topouzelis *et al*. (2004) using MLP and RBFs. In these studies, results which were based in a single image were presented.

The general objectives to this work have been to test the potentiality of feed-forward artificial NNs for oil spill detection using full resolution SAR satellite images. Two well known feed-forward networks, the MLP and the RBF, were examined to evaluate their performance in distinction between oil spills and look-alikes. The main aim of the present work is to detect the most suitable network and training algorithm, the best topology for this network and the data structure, which best fits our classification problem. The term topology refers to the structure of the network as a whole, specifying how its input, output and hidden units are inter-connected.

2. Neural networks related theory

2.1 *Neural network architectures and training algorithms*

In the present study, two different feed-forward networks are tested to identify the one most suitable for oil spill detection: the MLP and the RBF networks. Both networks work in a supervised manner, are very good in classification and inversion problems, easy to use, work as universal approximators, have very good non-linearity capabilities and are the most used in the feed-forward network family (Bishop 1995). The Stuttgart neural network simulator (SNNS) was used to test the networks' capacity.

2.2 *MLP neural networks*

The most popular class of multilayer feed-forward networks is the MLP. The MLP usually comprises one input layer, one or two hidden layers and one output layer. As an example, a four-layer network with two hidden layers can be seen in Figure 1. The MLP is presented as very powerful in classification and inversion problems, it is easy to use, it works as a universal approximator, it has very good non-linearity capabilities and it is the most widely used. In the present study, input nodes correspond to pixel intensity values, hidden layers are used for computations and output layers correspond to the classes to be recognized.

There are several training algorithms for MLP. Four algorithms of the gradient descent family were examined: BP, Conjugate Gradient (CG), Resilient back propagation (Rprop) and Quick BP (Quickprop).

The BP algorithm tries to minimize the sum squared error (SSE) of the network adjusting the weights and the biases of the network. This is done by continuously changing the values of the network weights and biases in the direction of the steepest descent with respect to error (Bishop 1995).

The CG uses second order derivatives to minimize the goal functions of the variables. In general, it chooses an initial point on the error surface, takes an arbitrary direction and moves along it until it reaches the minimum in that direction. Subsequently, it takes a conjugate direction relative to the previous one and again it tries to reach the minimum on that direction.

Rprop is a local adaptive learning algorithm which eliminates the influence of the size of the partial derivative on the weight step. As a consequence, only the sign of the derivative is considered to indicate the direction on the weights update (Zell *et al*. 1993).

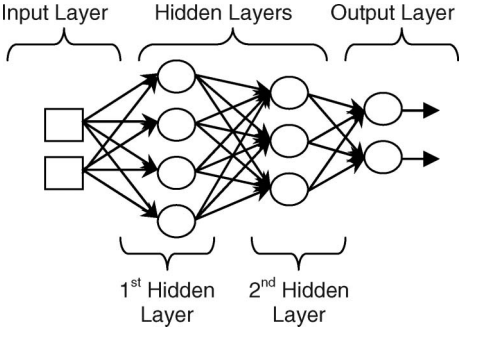

Figure 1. An example of MLP network.

Quickprop uses information about the curvature of the error surface. This requires the computation of the second order derivatives of the error function. The error surface is assumed locally quadratic and attempts to jump directly from a current position to the minimum of the parabola (Zell *et al.* 1993).

2.3 *RBF neural networks*

The RBF-NN, which is a fixed three-layer network, can be seen as a special class of multilayer feed-forward networks. Each unit in the hidden layer employs an RBF, such as the Gaussian Kernel, as the activation function. The output units implement a weighted sum of hidden unit outputs. The RBF (or Kernel) function is centred at the point specified by the weight vector associated with the unit. Both the positions and the widths of these kernels are obtained from training patterns. Each output unit implements a linear combination of these RBFs. Figure 2 illustrates the architecture of an RBF network. Coefficients μ_{ji} represent the centres of radial basis and w_{kj} are the weighting coefficients of the linear combination.

There are a variety of training algorithms for the RBF networks. In the present study, the dynamic decay adjustment (DDA) algorithm is used (Zell *et al.* 1993). The DDA algorithm uses a constructive training where new RBF nodes are added whenever necessary. It is characterised by fast training (because a few epochs are needed to complete the training) and guaranteed convergence (Zell *et al.* 1993). The main characteristic of the algorithm is that when a training pattern is misclassified, either a new RBF unit is introduced or the weight of an existing RBF is incremented.

The main difference in the way that the two neuron network models try to solve a classification problem is that MLP calculates hyper-planes to separate classes whereas RBF uses kernels to group pixels from the same class.

3. Dataset description

For the present study, a dataset of 12 full-resolution SAR images is used. The dataset contains several sea states and all images contain several dark areas. Ten of the images contain at least one oil spill, whereas the other two contain only look-alike formations. The images have been thoroughly analysed by visual photo-interpretation and have been used in several studies (Pavlakis 1995, Pavlakis *et al.* 2001).

An ERS scene ($\sim$120 Mb) requires 5 h for processing, whereas an image window of 4–16 Mb size, requires 2–5 min. Thus, the method was applied on image windows of 4–16 Mb. Because of the numerous different networks, the comparison of their

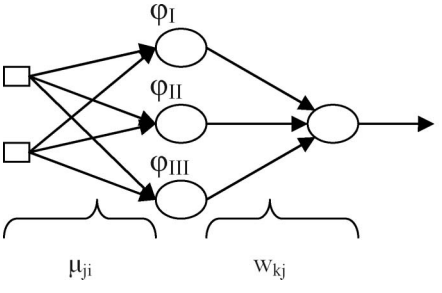

Figure 2. An example of RBF network.

performance was made using one SAR image window extracted from the ERS-1 image captured on 1 June 1992 (orbit 4589, frame 2961). This image presents a rough sea surface, sufficient to produce a strong contrast signal in the presence of oil spills. It also contains look-alikes in the left part, caused by a different sea state (local wind falls in a big swell wave). Then, the performance of the most appropriate network was further tested using the rest of the dataset to check its potential for the detection of oil spills of various age, shape, area and backscattering properties.

NNs need to be trained to perform a specific task. In the present study, we were concerned with only two categories: spilled area and non-spilled area. Thus, for the selected training image window, three quite small training areas were selected; one containing spilled area, one containing look-alike phenomena and a last one containing sea area. Each training area was of approximately 700 pixels, formatting in the end a training file with more than 2000 training inputs.

Analysis followed using 13 image windows extracted from the 12 aforementioned images. These image windows were also forming the testing test as they were evaluated in a later step with a reference dataset. Six of the image windows contained only dark formations caused by natural phenomena, i.e. fronts, wind shadow areas and low wind areas. Five of them contained different types of oil spills discharged by ships, i.e. fresh straight oil spills with or without tapered front, old angular oil spills with tapered front, broad distorted oil spills without tapered front and amorphous oil spills. The last two image windows contained both natural phenomena and oil spills. Image windows were carefully selected to contain different sea states and different dark formations, i.e. shape, area and texture. The selection of different sea states and dark formation types is crucial to ensure the networks' generalization ability.

Oil spills or look-alike phenomena do not have a certain size. Thus, there is not a window size that could be used to crop the SAR images. The size of the extracted widows varied according to the size of the dark areas. Image windows were extracted according to the rule that the surrounding of the dark phenomenon area should be approximately double the size of the dark area.

4. Methodology

The oil spill detection problem can be separated into two phases (Figure 3). Firstly, dark areas containing dark pixels need to be detected and secondly, these pixels have to be classified as part of an oil spill or not. The dark area detection phase is based on threshold techniques. The classification phase is made using NNs and statistical values derived from the original images. NNs use these values as inputs to classify the pixels as an oil spill or not.

4.1 *Dark areas detection – features extraction*

To incorporate this study into an integrated system, which is pixel based, NNs operate in a pixel basis environment. This environment was selected against other types, e.g. an object based environment, to avoid problems formatting from the grouping of pixels. The dark area detection phase was made using a two level threshold algorithm (Karathanassi *et al.* 2006). This threshold algorithm is very efficient in detecting dark areas on SAR images as it takes into consideration the pixel values in different resolutions.

After the detection of dark pixels, several images are generated from the original SAR, each one presenting a texture or geometry key-feature. In a previous study, an

investigation of the features contributing to oil spill detection has been performed (Topouzelis *et al.* 2002) and features, which have led to successful oil spill detection, have been selected. These are: the shape texture, the asymmetry, the mean difference to neighbours and the power to mean images (Figure 4). Shape texture refers to the texture which is based on spectral information provided by the SAR image and is calculated as the standard deviation of the different mean values of dark pixels containing in an area (i.e. dark area). Asymmetry can be expressed as the ratio of the lengths of the minor and major axes of an ellipse which can be approximated for each dark area. Mean difference to neighbours can be expressed as the mean difference for each neighbouring dark area multiplied by the shared border length of the areas concerned. Power-to-mean ratio is defined as the ratio of the standard deviation and the mean value of the areas.

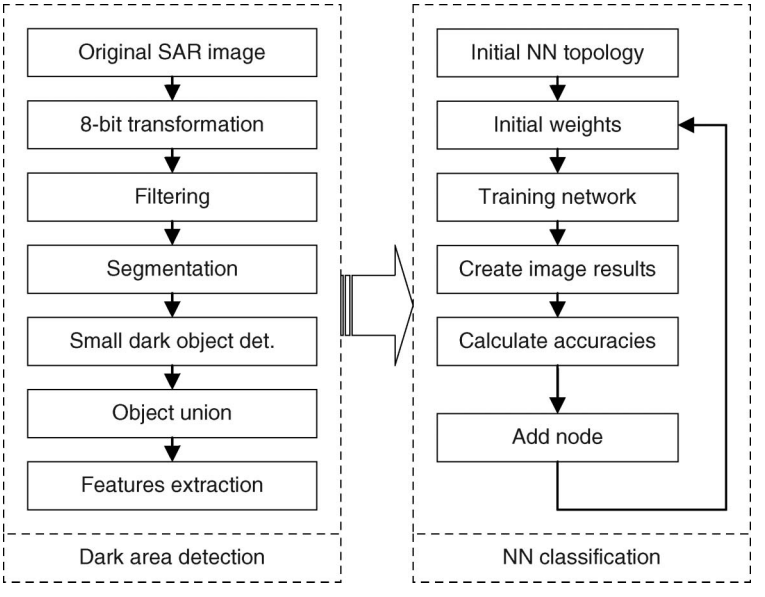

Figure 3. Flow diagram of the used methodology.

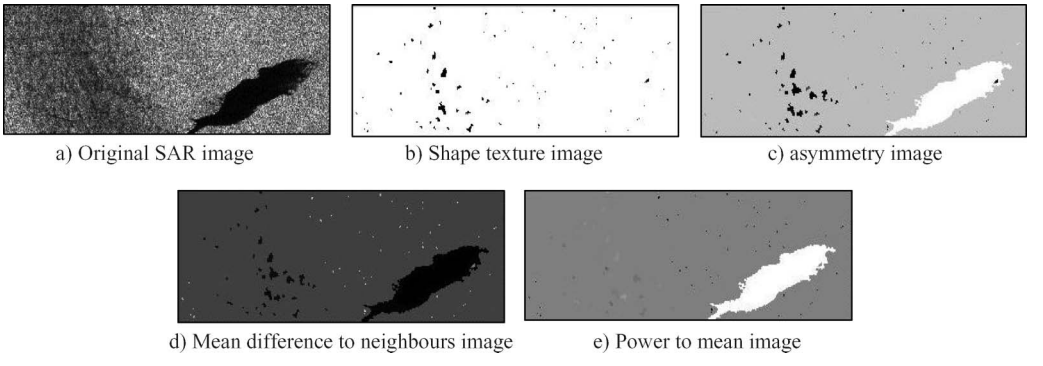

Figure 4. Inputs to feed forward neural networks.

4.2 *Neural network classification*

The second phase includes the classification of the dark areas as oil spills or look-alikes using NNs. The problem of oil spill detection through NN classification has five main aspects: network family selection, type and size of input data preparation, network topology selection, training algorithm decision, parameters estimation and finally network performance assessment. In previous paragraphs, the two selected network families were described. The following paragraphs are dedicated to the remaining aspects of the NN classification.

Data preparation was necessary in order for the values of the used features to meet the NN requirements. Preparing the data is mainly referred to as data normalization. Image values were transformed into a certain interval of values. Without this process any input unit with a large value will dominate the results. Normalization was performed with linear transformation of the images interval (0–255) to the NN interval (0–1). It is of high importance not to use the minimum and maximum values in each window for the image interval, as the final classification would be biased and the generalization would fail. Normalization was performed for all the image layers, i.e. images representing the selected features.

For both NN families an initial network topology was selected. The selection of the best suited topology for each network was designed through the hill-climbing approach, which uses as a search point a solution created from a previous topology. The contractive algorithm was used, in which the initial topology was the simplest one and nodes were added afterwards. The performance of each topology was evaluated and the process was repeated iteratively until a predetermined stopping criterion was achieved. The constructive algorithm easily specifies the initial network topology and it is significantly faster in terms of training time.

As initial network topology for MLP, the following was chosen: a layer with one input node (the original SAR image) and one output node. The process continued until a complicated network with five input nodes, two hidden layers with five and four neurons respectively and an output layer with one neuron were created. The nature of the RBF network requires a strictly three-layer network. A two-input network was initially selected but without luck, as the training algorithm had relatively good performance with 14 hidden units, which makes the classification procedure very complex. Afterwards, the three-input topology was examined using initially two hidden units. The process continued until the five-input topology with seven hidden units was created. In total, 41 and 18 networks of MLPs and RBFs respectively were created and tested (Figures 5 and 6).

During a NN's training, it is of high importance to specify the training parameters. These parameters define when training will stop and usually they refer to training epochs and/or to errors (differences between inputs and outputs). In the present study, as stopping criteria, 500 training epochs and 0.1 SSE (the sum of the quadratic differences between the teaching input and the real output over all output units) were defined. Practically, each network was trained for 500 epochs except if SSE reached the 0.1 value. If SSE was increasing for more than 100 epochs then the training procedure was stopped and the procedure was repeated until the minimum SSE value was encountered.

For the selection of the best topology, comparison between results and a reference dataset were implemented. a reference dataset was produced by photo-interpretation methods and techniques for the 13 image windows. Comparison was made using confusion matrices (Congalton and Green 1998).

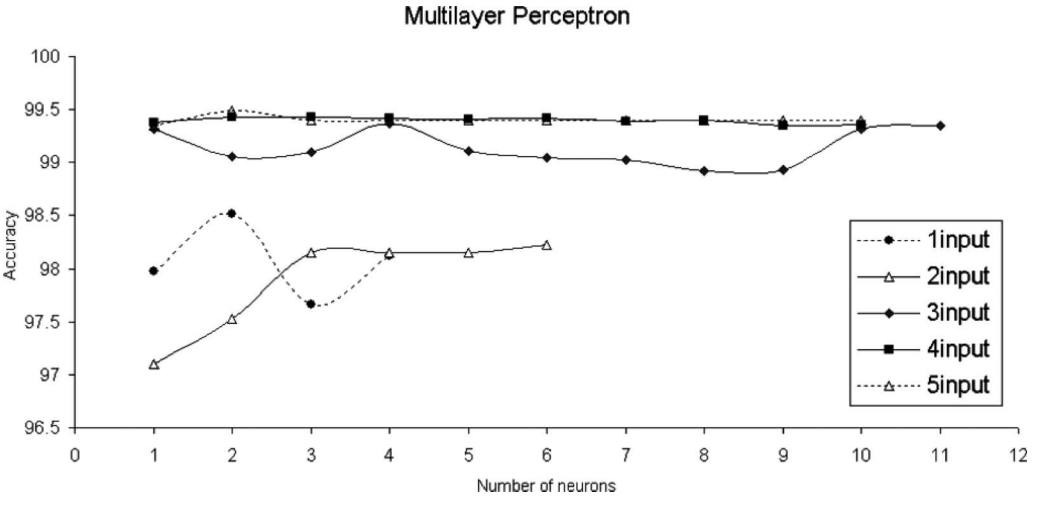

Figure 5. Classification performance of multilayer perceptron networks.

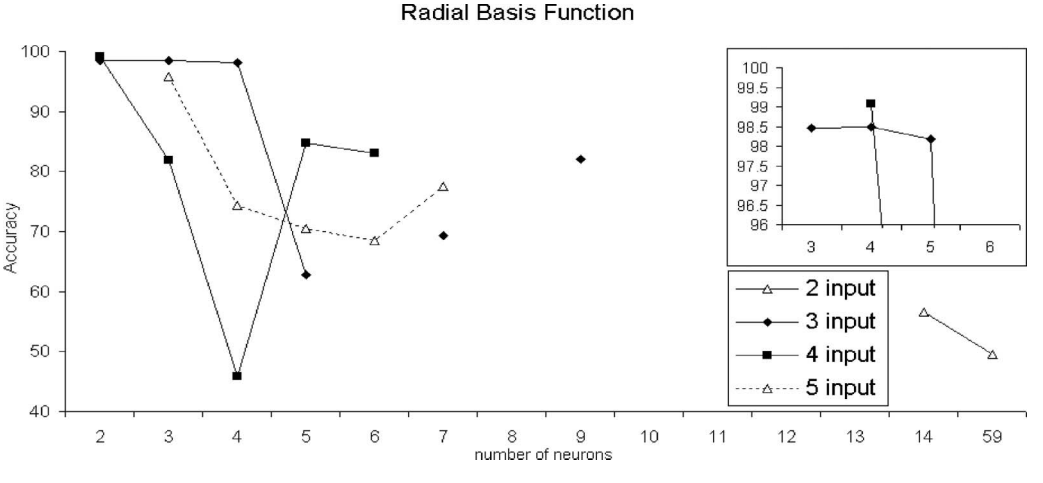

Figure 6. Classification performance of radial basis function networks.

For each produced image, the overall, oil spill and sea accuracy were calculated by means of the confusion matrix. Each network was tested on the same dataset consisting of 13 image windows. By averaging the 13 image window accuracies, the mean networks' accuracy was calculated. Overall accuracy was calculated by dividing the total number of the pixels correctly classified by the total number of the pixels of the images. Oil spill accuracy was calculated by dividing the pixels classified correctly as oil spill with the total number of the pixels referenced as oil spill. Sea accuracy was calculated similarly to dark formation accuracy, taking into account the total number of pixels referenced as sea area. Overall and sea accuracies were expected to present quite high values as the reference dataset mainly included large sea areas. Sea discrimination is not the main task of the present work; however, it is getting very crucial to detect oil spills correctly. Low sea

accuracy mainly represents dark formations which do not exist in reality and they can be considered as image noise. Oil spill accuracy had great importance as the number of pixels presenting oil spills was much smaller than that of the sea.

For the proposed topology, four training algorithms were investigated: BP, CG, quick propagation and resilient BP, to examine which one has the better performance.

All the necessary steps concerning NNs (creation, training and results production) were made using the SNNS v4.2 software. Where necessary (pre-processing, and network performance evaluation) ancillary programs were created using the IDL v6.1 language.

5. Experimental results

A comparison between the reference photo-interpreted datasets and the NN results follows. Because of the 13 image windows and numerous NN topologies, results are presented in terms of accuracy averages for the 13 image windows.

5.1 *Types and networks comparison*

Figure 5 presents the results of the different MLP network topologies categorized by input units. It can be seen that topologies with one (original SAR image) or with two input units (original SAR image and shape texture image) do not classify the image correctly. In contrast, topologies using more than two input units have a much better performance. If we concentrate on the latter, we can see that there is a special interest to topologies containing seven nodes (input-hidden-output). Also, if we investigate the performance of accuracy in terms of the existing neurons, we can assume that the topologies having the best performance are 3:3:1, 4:2:1, 5:1:1 (Table 1). Because of the fact that for each input node the size of the original data increases by 20% and the needs of computational time and power are significantly increased, the topology that is proposed is 4:2:1. The accuracy of this topology is strongly connected with the specific inputs as these are presented in paragraph 4.2. The proposed four input nodes topology, i.e. SAR image, shape texture, asymmetry and mean difference to neighbours, was proven to be the appropriate topology for classifying oil spills very accurately. Looking at the results of the five input nodes topology in detail, we noticed that the information in the borders of the oil spill was lost. Furthermore, more computational power and training time were needed.

Table 2 presents the performance of each training algorithm (BP, CG, quick propagation and Resilient BP) when the selected topology is used (Table 2). All the algorithms were tested regarding the required speed for approaching the desired error value. Moreover, their ability to reach global minima from different initial weight values

Table 1. Best network accuracies.

Network	Topology	Accuracy (%)
MLP	3:3:1	99.37
	4:2:1	99.43
	5:1:1	99.49
RBF	3:2:2	98.45
	3:3:2	98.48
	3:4:2	98.19
	4:2:2	99.08

Table 2. MLP algorithm performance.

Algorithm	Speed	Local minima avoidance
Backprop	Slow	Yes
CG	Fast	No
Quickprop	Fast	No
Rprop	Medium	Yes
Backprop-CG	Fast	Yes

was also examined. BP as the standard algorithm for the feed-forward networks works generally well, but it is very slow. A big number of interactions are needed to be sure that the network has been trained well. In contrast, CG works very quickly, a few interactions are needed but many times they get stuck in local minima and cannot reach the global minima. Furthermore, Rprop works somewhere in the middle of the previous two, in terms of interactions and global minima reaching. Quick propagation in most cases diverges from the global minima and cannot find a solution. To speed up the training but to be sure that local minima are avoided, a hybrid algorithm can be used. Training can start using the BP algorithm (in the present study, 75 epochs) avoiding, in this way, the local minima, and afterwards the CG (25 epochs) is applied quickly to achieve the desired accuracy.

Figure 6 presents the results of different network topologies in terms of input units for RBF networks. We observe that their performance is lower than MPL. It starts from nearly 45% while only four topologies can be compared with the majority of MLP, which are above 95% (small window in Figure 6, Table 1). The topology with three input units is the only one with relative stability close to 98.5 and is limited from seven to nine nodes (3:2:2, 3:3:2, 3:4:2, 4:2:2). Better performance was observed for the 4:2:2 topology with 99.08%, whereas the performance of all the other topologies is under 99%. From the aforementioned, it can be concluded that from the feed-forward family the MLP network has a better performance in oil spill detection than the RBF network.

5.2 *Generalization ability*

The ability of the networks to preserve their performance with data never before used is crucial for our classification task. It refers to the ability of the networks to classify successfully different images containing oil spills and/or look-alikes. For this step, only the selected network with MLP – 4:2:1 topology was used.

A classified image identifying the oil spill presence was produced for the selected network topology for the 13 SAR image windows. For each produced image, a comparison with a reference dataset was made. A reference dataset was produced by photo-interpretation methods and techniques for the 13 image windows.

Figure 7 contains four examples of dark features, two of them identified as oil spills and two as look-alikes. It can be seen that the MLP network has quite good performance on the detectability of the oils spills. The overall accuracy of the MLP network for the 13 image windows examined was 96.46%. For the seven cases where image windows contain only oil spills or both oil spills and look-alikes, the oil spill accuracy was 91.35%. For the six cases containing only look-alikes, NN correctly classified 94.90% of the pixels.

Concerning the different types of black features and the variety of oil spills and look-alikes, the generalisation of the MLP – 4:2:1 topology can be considered very sufficient. The NN can distinguish very satisfactorily oil spills from look-alikes in most of the cases.

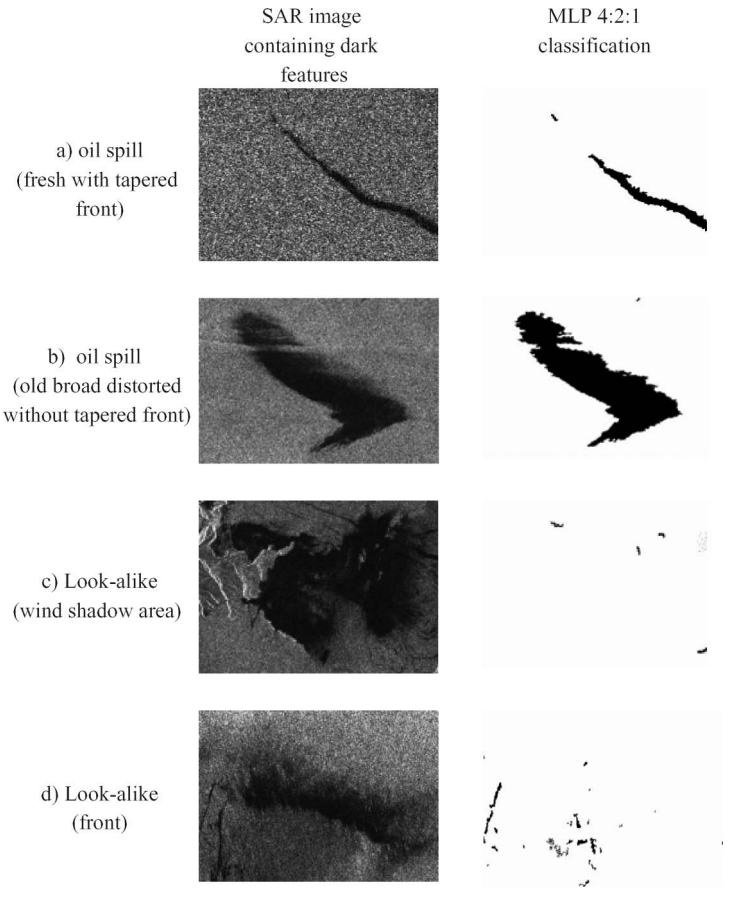

Figure 7. Results of dark feature classification by MLP 4:2:1 neural network.

Only small parts or very linear oil spills or small black linear natural phenomena were wrongly misclassified. Also, after the training, the classification results of the MLP – 4:2:1 network can be produced very quickly and the classification procedure does not take more than 5 min for each image window.

6. Conclusions – discussion

In this study, an investigation of the most appropriate feed-forward NN for distinguishing oil spills from look-alikes using full resolution SAR images was performed. Thirteen image windows have been used from 12 SAR images, six of them containing look-alikes, five oil spills and two both oil spills and look-alikes. Two types of NNs were used; the MLP and the RBF networks.

Training is more time consuming for MLP than for RBF. However, in RBF networks the initial location of the radial basis centres (which are described from the link weights between input and hidden layer) has to be selected very carefully, otherwise the RBF networks will not converge. For this reason it can be concluded that RBF networks are not as stable as MLP. Furthermore, MLP has a better generalization ability than RBF. From

the two feed-forward NN models examined, MLP works more reliably than RBF for oil spill detection.

Comparison was made using confusion matrixes between the photo-interpretation results and NN results. Overall accuracy was calculated by dividing the total number of the pixels correctly classified by the total number of the pixels of the images. The mean performance of an NN family was produced by averaging the performances of every examined topology of that family. The mean performance for all RBF topologies examined was 77.62%, whereas for MPL it was 98.98%. In conclusion, the MLP networks present two main advantages over RBF networks. They have better generalization ability in terms of accuracy measurement and they are more stable during the training session than RBF.

Several topologies were examined using the constructive method. The topology best suited for the classification procedure was the MLP 4:2:1 according to specific inputs. Classification accuracy was 99.433% for the above topology. The high performance of 4:2:1 MLP NN as classifier was confirmed by producing an overall accuracy of 96.46% when applied to other images that contain oil spills and look-alikes and had never before been introduced to the network. Therefore, the network generalization ability is considered to be sufficient.

NN's ability to successfully generate non-linear datasets, which have never been seen before, is a big advantage over the commonly used statistical approaches. Further research could include more images, other network categories and variations of the existing networks.

References

Bishop, C.M., 1995. *Neural networks for pattern recognition*. Oxford: Oxford University Press.

Congalton, R.G. and Green, K., 1998. *Assessing the accuracy of remotely sensed data: principles and practices*. Boca Raton, FL: Lewis Publishers.

Del Frate, F., Petrocchi, A., Lichtenegger, J., and Calabresi, G., 2000. Neural networks for oil spill detection using ERS-SAR data. *IEEE Transactions on Geoscience and Remote Sensing*, 38 (5), 2282–2287.

Ferraro, G., Tarchi, D., Fortuny, J., and Sieber, A., 2006. Satellite monitoring of accidental and deliberate marine pollution. *In*: M. Gade, H. Hóhnerfuss, and G.M. Korenowski, eds. *Marine surface films: chemical characteristics, influence on air–sea interactions, and remote sensing*. Heidelberg, Springer, 273–288.

Fiscella, B., Giancaspro, A., Nirchio, F., Pavese, P., and Trivero, P., 2000. Oil spill detection using marine SAR images. *International Journal of Remote Sensing*, 21 (18), 3561–3566.

Kanellopoulos, I. and Wilkinson, G., 1997. Strategies and best practice for neural network image classification. *International Journal of Remote Sensing*, 18 (4), 711–725.

Karathanassi, V., Topouzelis, K., Pavlakis, P., and Rokos, D., 2006. An object-oriented methodology to detect oil spills. *International Journal of Remote Sensing*, 27 (23), 5235–5251.

Kavzoglu, T. and Mather, P., 2003. The use of backpropagation artificial neural network in land cover classification. *International Journal of Remote Sensing*, 24 (23), 4907–4938.

Kubat, M., Holte, R.C., and Matwin, S., 1998. Machine learning for the detection of oil spills in satellite radar images. *Machine Learning*, 30 (2-3), 195–215.

Nirchio, F., Sorgente, M., Giancaspo, A., Biamino, W., Parisato, E., Ravera, R., and Trivero, P., 2005. Automatic detection of oil spills from SAR images. *International Journal of Remote Sensing*, 26 (6), 1157–1174.

Pavlakis, P., 1995. Investigation of the potential of ERS-1/2 SAR images for monitoring oil spills on the sea surface. Joint Research Centre, European Commission, Report EUR 16351 EN.

Pavlakis, P., Tarchi, D., and Sieber, A., 2001. On the monitoring of illicit vessel discharges, a reconnaissance study in the Mediterranean sea. European Commission, Report EUR 19906 EN.

Perkovic, M., Harsch, R., Suban, V., Vidmar, P., Nemec, D., Móllenhoff, O., and Delgado, L., 2008. The use of integrated maritime simulation for education in real time. *In*: *16th conference on maritime education and training*, 14–17 October, Izmir. Turkey.

Solberg, A., Storvik, G., Solberg, R., and Volden, E., 1999. Automatic detection of oil spills in ERS SAR images. *IEEE Transactions on Geoscience and Remote Sensing*, 37 (4), 1916–1924.

Stathakis, D. and Perakis, K., 2007. Feature evolution for classification of remotely sensed data. *IEEE Geoscience and Remote Sensing Letters*, 4 (3), 354–358.

Stathakis, D. and Vasilakos, A., 2006. Comparison of computational intelligence based classification techniques for remotely sensed optical image classification. *IEEE Transactions on Geoscience and Remote Sensing*, 44 (8), 2305–2318.

Topouzelis, K., Karathanassi, V., Pavlakis, P., and Rokos, D., 2002. Oil spill detection: SAR multi-scale segmentation and object features evaluation. *Proceedings of SPIE, Image and Signal Processing for Remote Sensing*, XII (6365), 77–87.

Topouzelis, K., Karathanassi, V., Pavlakis, P., and Rokos, D., 2004. Oil spill detection using RBF neural networks and SAR data. *In*: *Proceedings of 20th ISPRS Congress*, 12–23 July, Istanbul.

Zell, A., Mache, N., Hubner, R., Mamier, G., Vogt, M., Herrmann, K., Schmalzl, M., Sommer, T., Hatzigeorgiou, A., Doring, S., and Posselt, D., 1993. SNNS: Stuttgart neural network simulator, Tech. Rep. 3/93, Institute for Parallel and Distributed High Performance Systems, University of Stuttgart, Germany.

Ziemke, T., 1996. Radar image segmentation using recurrent artificial neural networks. *Pattern Recognition Letters*, 17 (4), 319–334.